# MEASUREMENTS OF PEROXIDES AND RELATED SPECIES DURING THE 1995 SUMMER INTENSIVE OF THE SOUTHERN OXIDANTS STUDY IN NASHVILLE, TN

J. B. Weinstein-Lloyd[1], J. H. Lee, P. H. Daum, L. I. Kleinman,
L. J. Nunnermacker, S. R. Springston, and L. Newman
Environmental Chemistry Division
Department of Applied Science
Brookhaven National Laboratory
Upton, NY  11973

October 1997
[Revised:  August 1998]

[1]    Chemistry/Physics Department, State University of New York, Old Westbury, NY  11568.

# Measurements of peroxides and related species during the 1995 summer intensive of the Southern Oxidants Study in Nashville, Tennessee

J. B. Weinstein-Lloyd

Chemistry/Physics Department, State University of New York, Old Westbury.

J. H. Lee, P. H. Daum, L. I. Kleinman, L. J. Nunnermacker, S. R. Springston, and L. Newman

Environmental Chemistry Division, Department of Applied Science, Brookhaven National Laboratory, Upton, New York.

**Abstract**. Hydroperoxide measurements are presented for 12 flights of the U.S. Department of Energy G-1 aircraft during the summer 1995 intensive of the Southern Oxidants/Middle Tennessee study. A three-channel analyzer, utilizing both peroxidase/$p$-hydroxy phenylacetic acid ($p$OHPAA) and ferrous sulfate/benzoic acid (FeBA) reagents permitted continuous measurements of hydrogen peroxide ($H_2O_2$), methyl hydroperoxide ($CH_3OOH$ or MHP), and hydroxymethyl hydroperoxide ($HOCH_2OOH$ or HMHP). The median concentration of total hydroperoxide was 5.2 ppbv, with median concentrations of 2.4, 1.7, and 0.97 ppbv for $H_2O_2$, MHP, and HMHP respectively. In the free troposphere, $H_2O_2$ concentration correlated with the concentration of its precursors, ozone, and water vapor. $H_2O_2$ profiles do not show elevated concentrations in the boundary layer, in contrast to vertical profiles of primary pollutants. The combination of high $NO_x$ concentrations that inhibited peroxide formation, and peroxide loss through deposition and reaction with OH, led to markedly lower peroxide concentrations within urban and power plant plumes. Photochemical calculations performed to estimate the magnitude of in-plume peroxide depression showed reasonable agreement with observations.

## 1. Introduction

Hydroperoxides are largely responsible for the aqueous-phase oxidation of atmospheric $SO_2$, resulting in formation of acid precipitation and visibility-reducing sulfate aerosol [*Penkett et al.*, 1979; *Lind et al.*, 1987; *Madronich and Calvert*, 1990; *Tanner and Schorran*, 1995]. The water solubility of hydroperoxides and their damaging effects in vivo suggest that hydroperoxide uptake by leaves may contribute to forest decline [*Masuch et al.*, 1986; *Becker et al.*, 1990; *Ennis et al.*, 1990]. When NO concentrations are low, peroxides are the principal sink for peroxy radicals that participate in tropospheric ozone formation [*Kleinman*, 1991; *Jacob et al.*, 199). High $NO_x$ (i.e., NO + $NO_2$) conditions favor the formation of $NO_x$ oxidation products, collectively referred to as $NO_z$. As such, peroxide concentrations and ratios of peroxide to $NO_z$ indicate whether ozone formation is limited by the availability of $NO_x$ or hydrocarbons [*Sillman*, 1995; 1997; *Kleinman et al.*, 1997].

Formation of hydrogen peroxide by the self-reaction of $HO_2$ radicals, and of organic hydroperoxides by the analogous reactions between $HO_2$ and $RO_2$ (where R may be any organic functional group), terminate the free-radical chain sequence initiated by ozone photolysis in the atmosphere. Laboratory experiments have shown the reaction of ozone with alkenes in moist air to be an additional source of $H_2O_2$ and hydroxyalkyl hydroperoxides via a nonradical pathway [*Becker et al.*, 1990; *Hewitt and Kok*, 1991; *Gäb et al.*, 1995]. Recent ground- and aircraft-based peroxide measurements, some using high pressure liquid chromatography (HPLC) to quantitate individual peroxides, have demonstrated that organic hydroperoxides can constitute a significant fraction of the total [*Hewitt and Kok*, 1991; *Enders et al.*, 1992; *Heikes et al.*, 1992; *Lee et al.*, 1993; *Weller and Shrems*, 1993, *Ayers et al.*, 1996, *MacDonald et al.*, 1995; *Fels*

and *Junkermann*, 1994; *Tremmel et al.*, 1994]. Although the formation of higher molecular weight hydroperoxides is expected to occur, $H_2O_2$, methyl hydroperoxide (MHP), and hydroxymethyl hydroperoxide (HMHP) are the major hydroperoxides so far identified in significant concentrations in the atmosphere [*Hellpointner and Gäb*, 1989; *Hewitt and Kok*, 1991]. Reliable measurements of individual hydroperoxides are necessary to validate our understanding of the mechanism of atmospheric photochemistry and the relative importance of competing oxidative pathways.

This paper describes hydroperoxide measurements aboard the DOE G-1 aircraft during the summer 1995 Southern Oxidants Study (SOS) intensive in Nashville, Tennessee. The Brookhaven National Laboratory three-channel continuous flow hydroperoxide analyzer was deployed for the first time from an aircraft during this study, yielding measurements of $H_2O_2$, MHP and HMHP. We present here some general features of the data, as well as analyses of individual flights. Companion papers discuss instrumentation and flights for the G-1 [*Hübler et al.*, this issue], ozone production rates (D. G. Imre et al., unpublished manuscript, 1998; L. J. Nunnermacker et al., unpublished manuscript, 1998), carbonyl measurements [*Lee et al.*, this issue] and the use of indicator species to discriminate between $NO_x$ and VOC-limited ozone production regimes [*Kleinman et al.*, 1997; *Sillman et al.*, this issue] (D. G. Imre et al., unpublished manuscript, 1998). The median concentration of total hydroperoxide in the boundary layer (BL) between 1100 and 1400 CDT (central daylight time) was approximately 5 ppbv, with more than 50% contributed by organic hydroperoxides. Inhibition of hydroperoxide production by high $NO_x$ concentration was evidenced by markedly lower hydroperoxide concentrations within urban and power plant plumes.

## 2.  Experimental

### 2.1.  Instrument

Hydroperoxides were determined with a three-channel continuous flow analyzer similar to the widely used Kok and Lazrus instrument [*Kok et al.*, 1986; *Lazrus et al.*, 1986], modified to permit analysis using Fenton chemistry for speciation of hydroperoxides. Ram air reached the instrument through 1 m of 3/8 inch ID Teflon® PFA tubing, mounted in a forward facing inlet on the side of the G-1. Figure 1 shows a schematic diagram of the instrument and identifies the species detected in each channel. Details of the analytical chemistry and solution composition for a similar ground-based instrument can be found in the papers by *Lee et al.* [1990, 1994]. Baselines were established several times during each flight by directing air through a Pd/alumina cartridge. Cartridge integrity was demonstrated by observing no change in the baseline when a second cartridge was placed upstream of the first.
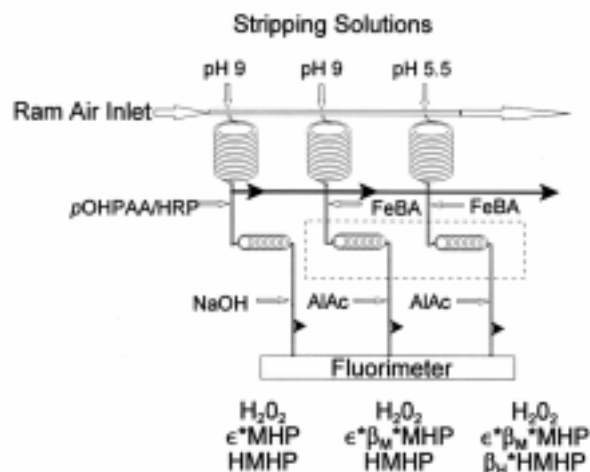


**Figure 1.** Schematic diagram of three-channel analyzer, showing *p*H of stripping solutions, fluorescence reagents (*p*-hydroxyphenyl acetic acid/horseradish peroxidase and Fe(II)/benzoic acid), fluorescence enhancing reagents (NaOH and Al(III)/acetate buffer), and species detected in each channel. The symbols ε, $\beta_M$, and $\beta_H$ denote the collection efficiency of MHP, and correction factors for detection of MHP and HMHP, respectively.

A two-point calibration was conducted before and after each flight using aqueous hydroperoxide standards, nominally 0.5 and 1.0 μM, prepared from unstabilized 3% hydroperoxide stock, with stripping solution used for the final dilution. Stock hydroperoxide was titrated against standardized permanganate before and after the 30-day measurement period, and the observed 1.5% decrease in concentration was assumed linear throughout the period. Nominal liquid and air flow rates, 0.32 mL/min and 1.5 L/min, respectively, were calibrated regularly. The 0 to 90% response time of the instrument was 110 s.

### 2.2.  Data Handling

Measurements are reported for 12 flights between July 2 and 20, 1995, each between 3 and 4 hours in duration. Approximately 80% of the data were collected between 0900 and 1500 CDT, within 110 km of the Nashville urban center. The initial data set employed for analysis consisted of 1 s points averaged to 10 s intervals. Because much of the data analysis planned involved comparison of hydroperoxide concentrations to those of other species, we were concerned about relative time responses. While most instrument response times were shorter than 30 s, the hydroperoxide instrument had a 110 s exponential response, the result of liquid mixing in reaction coils and fluorescence cells. We applied an exponentially weighted averaging algorithm to measurements from the faster instruments to match their response times to hydroperoxide; it is this time-averaged set of 10 s data points which is used for the analysis described herein. Because the analysis of clear air data was the goal of this study, an attempt was made to avoid flights through clouds. Examination of correlations between trace gas species was conducted on a data subset screened to remove measurements made in air containing cloud droplets (coarse particle count >10 cm$^{-3}$); these amounted to <4% of the data points. Gaps in data shown below reflect periods during which zeros and calibrations were performed. All times in the following discussion are central daylight time (CDT + 5 hours = GMT).

### 2.3.  Error Assessment and Hydroperoxide Speciation

Uncertainty in determining individual hydroperoxide concentrations arises from indeterminate errors in standard calibrations and hydroperoxide collection efficiencies as well as fundamental questions about the response of each channel to specific hydroperoxides. The detection limit for $H_2O_2$ in each channel is 100 parts per trillion by volume (pptv), reported as 3σ for a baseline on the ground. For a single channel the uncertainty in converting aqueous-phase standards to gas-phase concentrations, including errors in determining liquid and air flow rates and stock hydroperoxide concentration, temperature variation, and evaporative losses, typically amounts to 15%. The reported uncertainty in the Henry's law constant for MHP is 12% [*Lind and Kok*, 1994], which translates into an uncertainty of 20% in collection efficiency ε. These considerations generate a ±30% error for the concentrations of individual hydroperoxides. Additional error is contributed by correction factors for partial detection of MHP and HMHP in the FeBA channels, which we determine using standard mixtures of these species. Standard composition is determined using HPLC with fluorescence detection after postcolumn derivatization using *p*-hydroxyphenylacetic acid/horseradish peroxidase (*p*OHPAA/HRP) reagent [*Hellpointner and Gäb*, 1989]. Correction factors, symbolized by ß$_M$ and ß$_H$ in Figure 1, were 0.4 and 0.2, respectively, and were reproducible within 2%. The validity of this procedure is based on the assumption that *p*OHPAA/HRP reagent is equally sensitive to all hydroperoxides, and that individual hydroperoxides exhibit the same relative stability in the HPLC and continuous flow systems. The assumption that no hydroperoxides are collected other than $H_2O_2$, MHP, and HMHP is another potential source of error. Any water soluble higher

hydroperoxide will generate a fluorescent dimer in the $p$OHPAA/HRP channel and will be reported as MHP or HMHP, depending on its stability toward hydrolysis at high $p$H [*Lee et al.*, 1994].

## 3. Results

### 3.1. Overview of the Data

Air chemistry in the Nashville area is influenced by urban emissions, coal-fired power plants, and biogenic hydrocarbons from surrounding agricultural land and forests. During the measurement period, meteorological conditions varied from clean northwesterly flow to stagnant high-pressure conditions conducive to the buildup of high concentrations of $NO_x$, ozone, and other pollutants. Though these conditions make it more sensible to interpret measurements obtained during individual flights, some features of the data set as a whole are worth noting. Total hydroperoxide concentrations were quite high, as was the proportion of organic hydroperoxide. For the entire data set, the median concentration of total hydroperoxide was 5.2 ppbv, with median concentrations of 2.4, 1.7, and 0.97 ppbv for $H_2O_2$, MHP, and HMHP, respectively. Composite vertical profiles, constructed from all 12 flights of the G-1, approximately 13,500 data points, are shown in Figure 2. The profiles show significantly higher median concentrations of accumulation mode aerosol particles (ACP), $SO_2$, CO, $NO_x$, $NO_y$ (i.e., $NO_x+NO_z$) and $O_3$ below 1500 m, consistent with sources in the BL. The $H_2O_2$ profile is more uniform, consistent with the absence of primary sources and inhibition of secondary formation in the region due to high $NO_x$ concentrations, as discussed below. The proportion of organic hydroperoxide (ROOH = MHP + HMHP) is large compared to previous summer aircraft measurements in Halifax and Ontario [*Macdonald et al.*, 1995; *Weinstein-Lloyd et al.*, 1996a] and winter measurements over the U.S. East Coast [*Barth et al.*, 1989], but similar to recent measurements over the eastern United States and the South Atlantic [*Tremmel et al.*, 1994; *Heikes et al.*, 199].

We examined a subset of the BL data collected during the period of peak photochemical activity, i.e., between 1130 and 1430. Fifty-one percent of the measurements were recorded during these hours, and of these, 71% were recorded at altitudes below 1500 m; 36% met both criteria. Median concentrations of $H_2O_2$ and MHP, 1.9 and 1.5 ppbv, respectively, were lower than the medians for all data, and HMHP, 1.0 ppbv, was unchanged. Figure 3, illustrating the range of hydroperoxide concentrations observed during these midday, BL flight segments, shows the highest concentrations generally to have occurred during the period from July 11 through July 17. This period is also associated with high temperature, humidity, and ozone concentrations.

Previous studies have shown that $H_2O_2$ concentration depends on the concentration of its precursors, $H_2O$ and $O_3$, in the free troposphere (FT), where $NO_x$ concentrations are low and hydroperoxides are not lost to deposition [*Daum et al.*, 1990; *Tremmel et al.*, 1993; *Weinstein-Lloyd et al.*, 1996]. This relationship is illustrated in Figure 4 for the composite set of FT data (altitude >1500 m). The regression line does not pass through the origin, as this simplified view of ozone production ignores the dependence of OH concentration on radical production rate and the dependence of $H_2O_2$ lifetime on OH concentration. The slope, 0.0045 ppbv/ppmv$^2$, is similar to summer
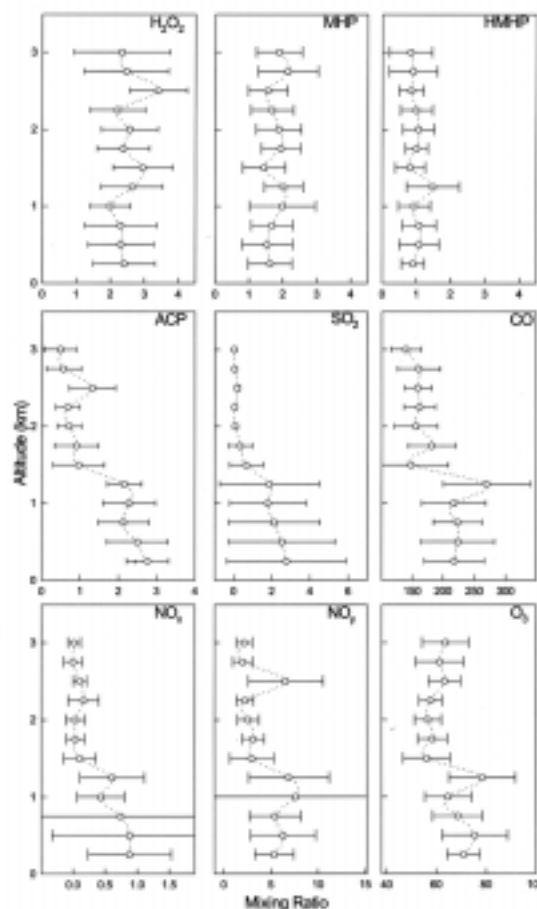


**Figure 2.** Composite vertical profiles of peroxides and related species. Abscissa units are parts per billion by volume (ppbv) for all species except ACP, $10^3$ cm$^{-3}$. Data shown for 250 m altitude bins. Circles indicate median values, and bars show interquartile range for each bin. Number of points per bin, beginning with the lowest altitude: 600, 3300, 1920, 210, 630, 230, 420, 120, 230, 510, 150, 580.

measurements in Halifax, Nova Scotia [0.0054 ppbv/ppmv$^2$; *Weinstein-Lloyd et al.*, 1996a] and over the northeastern U.S. [0.0050 ppbv/ppmv$^2$; *Tremmel et al.*, 1993]. The correlation is largely driven by water vapor concentration, which varied by a factor of approximately 40 for this data subset, rather than by ozone, which varied by only a factor of 3.

Competition between $HO_2$ and NO for reaction with $HO_2$ favors formation of $HNO_3$ over $H_2O_2$ in plumes, but one would not expect the composite data set to show a strict anticorrelation between the latter species because of differences in their formation rates and background concentrations. A decrease in hydroperoxide concentration is observed consistently within plumes, however, as shown in Figure 5. These traces, for the flight of July 11, show several plumes of elevated $NO_x$ concentration between 14.6 and 15.8 CDT. Coincident with each plume traverse is a depression in hydroperoxide mixing ratio. Because plume chemistry acts only as a perturbation to background hydroperoxide levels, we investigated the dependence of
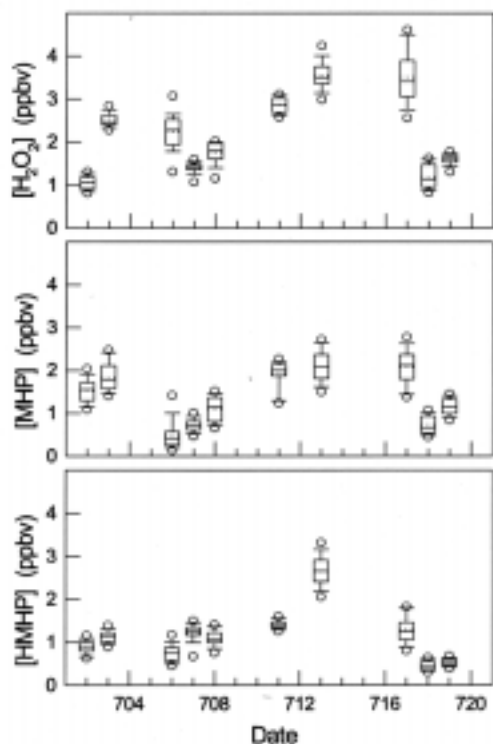
**Figure 3.** Peroxide distributions for midday, boundary layer flight segments. Rectangles enclose 50% of the data; means and medians are indicated by dashed and solid lines, respectively, and circles indicate 5th and 95th percentile points.
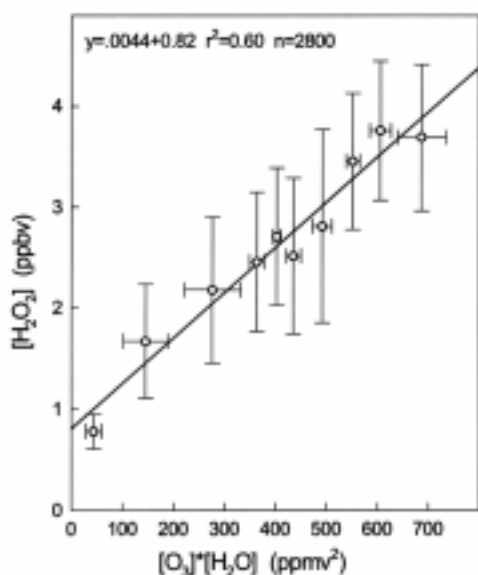


**Figure 4.** Production of $H_2O_2$ from precursors in the free troposphere. Data collected for alt >1500 were aggregated into 10 bins in order of increasing values of $O_3 \cdot H_2O$, each containing 10% of the data. Symbols represent mean of each population; standard deviation shown by horizontal and vertical bars.
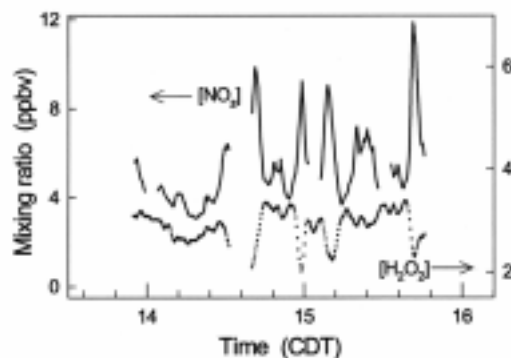


**Figure 5.** Anticorrelation between peroxide and $NO_z$ in plumes for July 11. $H_2O_2$, dotted line; $NO_z$, solid line.

observed hydroperoxide concentrations on wind direction. Much of the data set was unsuitable for this analysis, because winds were either too weak for their direction to be characterized or shifted during the measurement period. However, consistent (>2 m/s) southwesterly winds prevailed during midday in BL air on July 3, 6 and 20, and similar winds were from the north and/or northwest on July 2, 7, 18, and 19. Median concentrations of all hydroperoxides were higher in air originating from the south (Table 1), as were the concentrations of $NO_y$, $NO_z$, CO, and total hydrocarbons, although there was no significant difference in temperature or water vapor concentration. Elevated $SO_2$ concentrations in northerly winds probably reflect emissions from power plants, which are concentrated north of Nashville. Higher concentrations of hydroperoxides and $NO_z$ probably reflect more intense photochemical activity in southern regions, as these species have a lifetime of several days in the absence of deposition. Despite higher total hydroperoxide concentrations in southerly air, there was no significant difference in the fraction of organic hydroperoxide (52% S versus 55% N).

**Table 1.** Trace Gas Concentrations for Air Masses Originating S/SW and N/NW of Nashville

| Species | S/SW Winds | N/NW Winds |
|---|---|---|
| Total peroxide | 5.09 | 2.89 |
| $H_2O_2$ | 2.44 | 1.28 |
| MHP | 1.60 | 1.02 |
| HMHP | 1.05 | 0.59 |
| CO | 289 | 187 |
| $SO_2$ | 0.86 | 2.32 |
| Total hydrocarbon | 6.42 | 3.01 |
| isoprene | 0.49 | 0.043 |
| Temperature | 20.8 | 22.0 |
| Water vapor | 11.8 | 11.4 |
| ACP | 2.24 | 2.50 |
| $O_3$ | 72.6 | 68.4 |
| $NO_x$ | 0.47 | 0.62 |
| $NO_y$ | 7.03 | 5.66 |
| $NO_z$ | 6.59 | 4.90 |

Units are ppbv except for temperature (˚C), water vapor (g/kg), and accumulation mode particles ($10^3$ $cm^{-3}$). S/SW wind column includes data collected between 1130 and 1430 for altitude <1.5 km on July 3, 6, and 20. N/NW wind column similar data collected on July 2, 7, 18, and 19.

## 3.2. Breakup of Nocturnal Boundary Layer

Flights to probe changes in the structure and chemical composition of the atmosphere upon breakup of the nocturnal BL were scheduled on two weekdays, July 12 and July 20. On both flights the G-1 repeatedly traversed a SW/NE path upwind of Nashville at three fixed altitudes, 210, 500, and 625 m. The increase in BL height between 0730 and 1130 is illustrated along with the flight profile for July 20 in Figure 6, which shows the earliest flight legs conducted above (A), and later portions within the BL (B). Concentrations of hydrogen peroxide consistently were lower within the mixed layer than above (median $H_2O_2$ =2.0 ppbv for B and 2.7 for A in Figure 6), while concentrations of MHP (2.2 ppbv above versus 2.1 ppbv within) and HMHP (0.9 above and within) were not significantly different. We attribute the difference in $H_2O_2$ concentration to overnight deposition on wet surfaces, in accord with its high solubility and observations that ground level concentrations generally approach zero overnight [*Kok et al.,* 1990; *Lee et al.,* 1993; *Das and Aneja,* 1994]. The smaller Henry's law coefficient of MHP and correspondingly lower deposition to wet surfaces may explain its lack of variability. Like $H_2O_2$, HMHP is highly soluble [*Zhou and Lee,* 1992] and will deposit overnight. However, formation of this species through ozonolysis of alkenes will exhibit a diurnal profile that differs from a radical formation process, depending on temperature through the rate coefficient as well as the temperature-dependent emission rate of biogenic alkenes [*Guenther*, 1993]. These complications and the low concentrations observed make it difficult to interpret HMHP abundances. Ozone and CO, with low water solubility, did not exhibit significant variability (73.6 ppbv above versus 74.2 ppbv within and 193 ppbv above versus 203 ppbv within, respectively). $HNO_3$, the principal component of $NO_z$, has a deposition velocity similar to $H_2O_2$ and is also significantly lower within the BL (4.4 versus 5.1 ppbv). Although we did not measure ground level hydroperoxides, the aircraft measurements confirm that nighttime losses are limited to a region very near the surface and clearly illustrate the existence of the long-lived hydroperoxide reservoir that contributes the background for the next day's photochemistry.

## 3.3. Individual Day Case Studies

**3.3.1. July 2, 1995.** On July 2, the G-1 flight probed the BL structure and chemical composition of air surrounding the Nashville urban area during the afternoon. The weather was cool and dry due to a high-pressure center north of Nashville, with very light winds. Only small peaks in $O_3$ and CO from the urban area were evident on the diagonal transect near the city, and there were no significant increases in $O_3$, $NO_z$, or CO during the 3.5-hour Sunday flight. This day was unusual in that concentrations of MHP exceeded those of $H_2O_2$, both nearly doubling in 4 hours, from 0.9 to 1.6 ppbv for $H_2O_2$ and from 1.2 to 2.5 ppbv for MHP. HMHP concentration remained close to 1 ppbv. Vertical profiles in Figure 7, taken around 1500, show a temperature inversion at 1.8 km, and water vapor and ozone profiles indicate a well-mixed BL below 1.5 km. BL concentrations of the three hydroperoxides are also fairly constant, with $H_2O_2$ and MHP increasing and HMHP decreasing with altitude in the FT. The decline with altitude of the HMHP mixing ratio is consistent
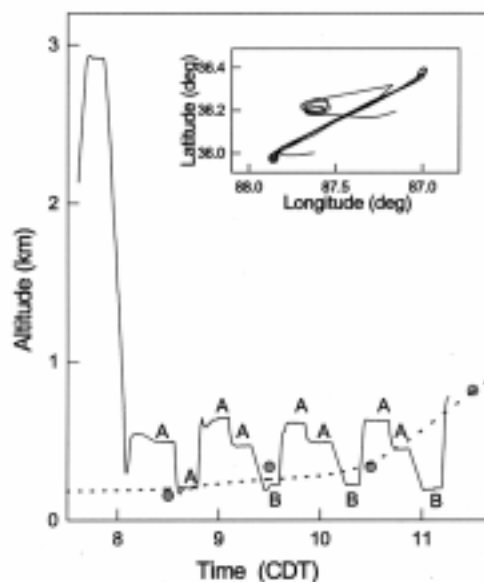


**Figure 6.** Altitude sequence for nocturnal boundary layer flight on July 20. A smooth line has been drawn through circles indicating the BL height at Dikson (latitude 36.2, longitude 87.4), obtained from the UAH website. Segments indicated by A were above, and B within the boundary layer. Inset shows the G-1 flight path.
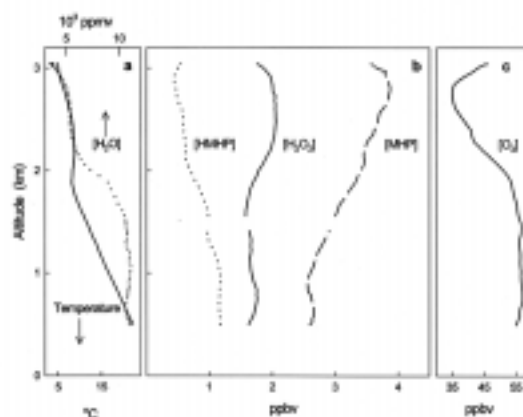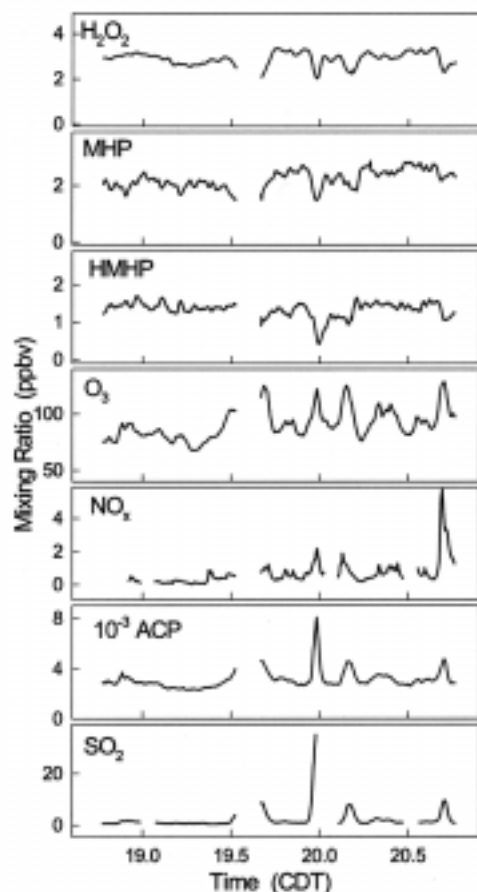


**Figure 7.** Vertical profiles on July 2 at 1500. (a) temperature, solid line; $H_2O$, dotted; (b) $H_2O_2$, solid line; MHP, dashed ; HMHP, dotted ; (c) $O_3$, solid line.

with a terrestrial source for this species in the ozonolysis of biogenic alkenes, while the similarity in $H_2O_2$ and MHP profiles is consistent with their free radical formation mechanisms.

**3.3.2. July 11, 1995.** July 11, a hot day with very light northeasterly winds, was part of a 4-day ozone episode [*McNider et al.,* this issue]. After an initial spiral, the G-1 flew at constant altitude (650 m) around the downtown area during mid-afternoon, encountering fairly high background pollution from the urban area ($O_3$ ~70 ppbv, $NO_y$ ~5 ppbv, and $NO_x/NO_y$ <0.1) and passing through plumes of elevated $O_3$, $NO_x$, and

particles, mostly associated with power plants, as indicated by high concentrations of $SO_2$ (Figure 8).  Boundary layer hydroperoxide concentrations remained fairly constant at 3.0, 2.2, and 1.4 ppbv for $H_2O_2$, MHP, and HMHP, respectively, except for traverses through plumes, where concentrations of all species decreased by up to 1 ppbv.

**Table 2.**  Correlation Between $O_3$ and $NO_z$ $+2 \cdot H_2O_2$

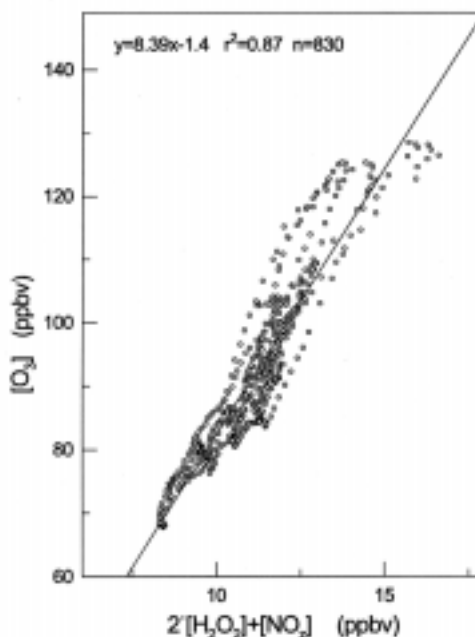| Date | Slope, ppbv/ppmv$^2$ | Intercept, ppbv | $r^2$ (Number of Data Points) |
|------|------|------|------|
| July 11 | 8.39 | -1.4 | 0.87 (  830) |
| July 12 | 7.00 | -2.4 | 0.59 (1170) |
| July 13 | 7.59 | -6.7 | 0.78 (  980) |



**Figure 8.**  Concentrations of trace gases on July 11.  All concentrations are in ppbv except for accumulation mode particles (ACP) in particles per cubic centimeter ($cm^{-3}$).



**Figure 9.**  Correlation between $O_3$ and $2 \cdot H_2O + NO_z$ on July 11.

A linear relationship between $O_3$ and the quantity $NO_z + 2 \cdot H_2O_2$, where $NO_z = NO_y - NO_x$,  has been noted by *Sillman* [1995] and *Sillman et al.* [this issue].  This correlation emphasizes the balance between radical sources and sinks and exhibits a slope that varies little between $NO_x$ and VOC-sensitive environments.  Sillman exercised the University of Michigan photochemical model to predict trace gas concentrations for the afternoon of July 13 [*Sillman et al.,* this issue].  Calculated $O_3$ varied linearly with $NO_z + 2 \cdot H_2O_2$, and the slope and intercept agreed reasonably well with observations.  Measured $O_3$ and $NO_z + 2 \cdot H_2O_2$ were not well correlated for all flights during the Nashville program, but data from July 11, 12 and 13 showed strong correlations with similar slopes and intercepts (Table 2), as illustrated for July 11 in Figure 9.  These observations can be attributed to stagnant conditions, which

minimized deposition and mixing of different air masses.  A similar strong correlation between these quantities was observed for measurements during the 1993 North Atlantic Regional Experiment in Halifax, Nova Scotia [*Weinstein-Lloyd et al.,* 1996a].  There, air was isolated from the surface by a low-level temperature inversion, and sampled air contained the products of several days' photochemistry.  Although NARE measurements were not characterized by calm winds, conditions were similar to the July 11-13 period in Nashville in that measurements were made on air masses that had retained the products of ozone photolysis.

**3.3.3.  July 13, 1995.**  Between 1300 and 1400 on July 13, the G-1 flew the perimeter of a 50 x 50 km box around Nashville.  Continuing stagnation on this day resulted in median air temperatures of 27.5°C at 1.2 km and 32.5°C at 700 m, and by 1330, median BL concentrations of $NO_y$, total hydroperoxides, and $O_3$ were 5.7, 8.4, and 90 ppbv, respectively.  Median concentrations of MHP and HMHP, 2.3 and 2.6 ppbv, represented 58% of total hydroperoxides.  The validity of the unusually high HMHP measurement, more than twice the median for any other flight (Figure 3) is supported by an  intercomparison with the NOAA P-3 aircraft earlier in the day, which showed good agreement for concentrations of total organic hydroperoxide [*Weinstein-Lloyd et al.,* 1996b].  Because HMHP
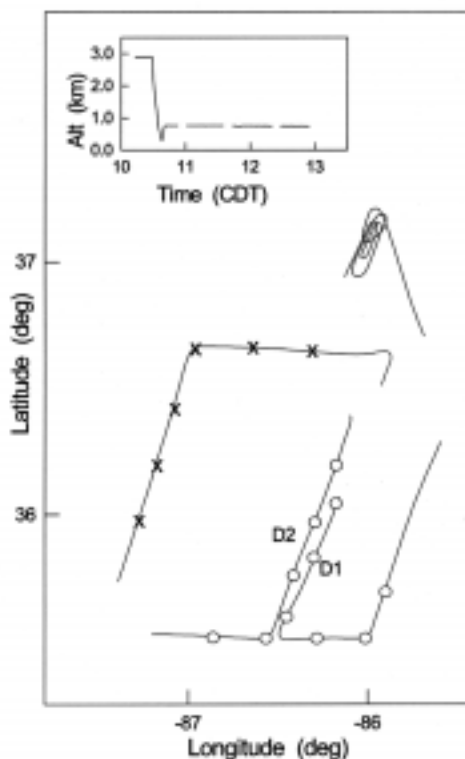
may be produced from the reaction between isoprene and ozone in the presence of water vapor, and isoprene emissions increase exponentially with temperature [*Guenther et al.,*1993, *Martin et al.,* 1991], it is tempting to ascribe the July 13 high HMHP to elevated temperature and concentrations of these precursors. However, the origin of elevated HMHP concentrations must be more complicated, as there is no obvious relationship between these quantities for other flights.

A vertical profile at 1430 showed a dry layer near 1.4 km sandwiched between two more humid layers (Figure 10).  Figure 10*c* shows a region near 1 km where $O_3$ is removed by titration with NO from the Johnsonville power plant plume ($SO_2$ >50 ppbv).  $H_2O_2$ profiles frequently exhibit maxima near the top of the BL [*Daum et al.,*1990; *Heikes et al.,* 1992, *Tremmel et al.,* 1993], which are attributed to reduced production rates in the drier FT and reduced concentrations in the BL due to deposition. The profiles in Figure 10b show a more complex structure. Above 1.5 km, profiles of all three hydroperoxides paralleled those of  water vapor and ozone (Figure 10b), in keeping with formation from free-radical precursors.  While $H_2O_2$ and MHP were fairly well mixed below 1 km, HMHP concentration decreased with altitude.  It is interesting to note that at the highest altitudes, the MHP mixing ratio was nearly twice its value at 500 m, while that of $H_2O_2$ was almost the same.  Lower nonmethane hydrocarbon (NMHC) concentrations in the FT may facilitate reaction of OH with $CH_4$, favoring the formation of $CH_3O_2$, the precursor to MHP.  The observed increase in HMHP concentration at high altitude suggests the existence of a free-radical formation pathway in addition to the ozone-biogenic alkene reaction, which is expected to occur near the ground.  A possible source is the radical $HOCH_2O_2$, formed by the reaction of formaldehyde with $HO_2$, which would produce $HOCH_2OOH$ by reacting with $HO_2$.



**Figure 11.**  Flight track for July 17.  Crosses and circles indicate upwind and downwind air, respectively, used to calculate median $H_2O_2$.  Inset shows altitude sequence.



**Figure 10.**  Vertical profiles of peroxides and related species at 1230, July 13.  (a) temperature, solid line; $H_2O$, dotted; (b) $H_2O_2$, solid line; MHP, dashed; HMHP, dotted; (c) $O_3$, solid line; $NO_y$, dotted.

**3.3.4.  July 17, 1995.**  Between 1030 and 1300 on July 17, the G-1 flew near downtown Nashville in a 90 x 100 km region around an altitude of 750 m (see flight pattern, Figure 11).

Median total hydroperoxide concentrations upwind of the city exceeded those downwind by 30% (7.57 versus 5.26 ppbv), with approximately half contributed by $H_2O_2$ and half by ROOH both upwind and downwind.  Median $H_2O_2$ concentrations were nearly equal (2.70 and 2.65 ppbv) on the two downwind legs (D1 and D2 in Figure 11) traversed approximately 1 hour apart, possibly because of compensating effects of photochemical production and dry deposition.  Sharp peaks in $SO_2$ and $NO_x$ indicate where the Gallatin and Cumberland plumes were sampled (G and C in Figure 12).  Decreased $H_2O_2$ and ROOH within plumes at 11.8, 12.2, and 12.9 hours are again evident.  It is especially interesting to note the anticorrelated hydroperoxide and $NO_x$ peaks at 12.2 hours in the Cumberland power plant plume.  Since the installation of efficient $SO_2$ scrubbers in 1994, Cumberland shows the lowest $SO_2$ emission rate (26 kton/yr) and lowest $SO_2$ to $NO_x$ ratio (0.22) of the four plants in the vicinity of Nashville.  The observed anticorrelation between $H_2O_2$ and $NO_x$ in the Cumberland plume (Figure 13)  despite relatively low concentrations of $SO_2$, dispels any notion that in-plume hydroperoxide dips are a sampling artifact from high $SO_2$. In contrast to July 13, there is poor correlation between $O_3$ and the measure of radical termination products, $NO_z+2\cdot H_2O_2$, possibly because of prior deposition of these species from the air mass.

**3.3.5.  July 18, 1995.**  A weak cold front passed on July 18, bringing lower temperatures and steady N/NE  winds (~5 m/s) to the region.  The G-1 flew three crosswind transects within the BL between 1100 and 1330, one upwind and two downwind of
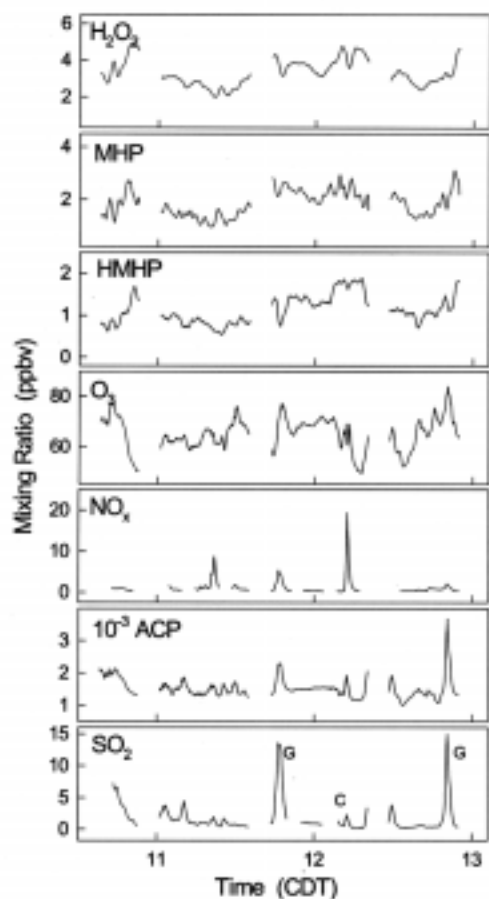
**Figure 12.** Concentrations of trace gases on July 17. All concentrations are in ppbv, except ACP in particles per cubic centimeter. Peaks attributed to Cumberland and Gallatin plumes indicated by C and G.
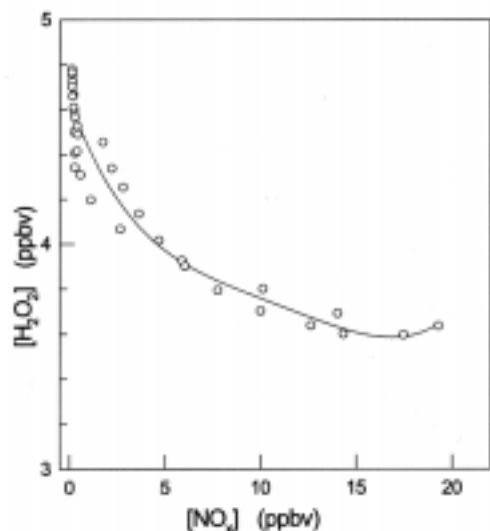


**Figure 13.** Anticorrelation between $H_2O_2$ and $NO_x$ in the Cumberland plume at 1210, July 17 (point C in Figure 12).

the urban center (UP, EW1, and EW2 in Figure 14). Each downwind transect sampled air at 310, 470, and 620 m, as indicated in the inset. Figure 15 shows trace gas concentrations for the flight. Particle and $SO_2$ emissions from the Gallatin power plant were observed at each altitude during the EW1 transect (G1, G2, and G3). The urban plume, distinguishable by peaks in $NO_x$ and particles without coincident $SO_2$, is indicated by Ur1, Ur2 and Ur3. Details of the urban plume chemistry for this day are discussed in the papers by L. J. Nunnermacker et al. (unpublished manuscript, 1998) and D. G. Imre et al. (unpublished manuscript, 1998).
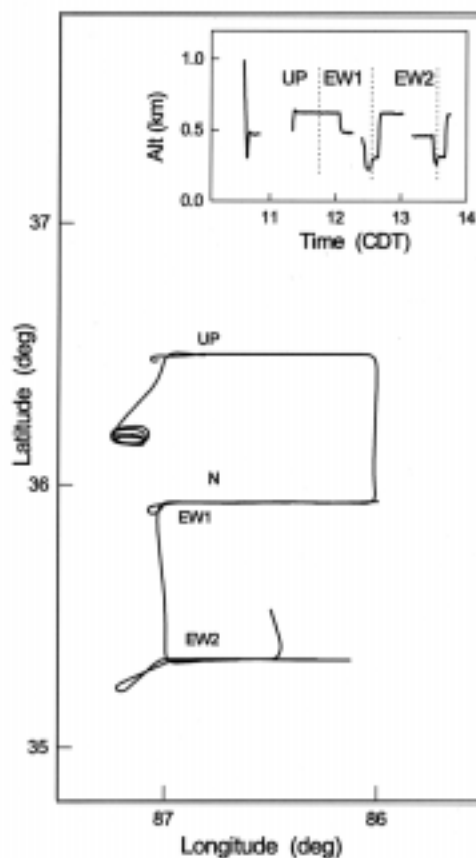


**Figure 14.** Flight track for July 18. Urban center indicated by "N", upwind and two downwind transects are indicated by UP, EW1, and EW2. Inset shows altitude sequence.

Within the BL the median concentration of total hydroperoxide was 2.2 ppbv, comprising approximately 51% $H_2O_2$, 29% MHP, and 20% HMHP. Examination of each hydroperoxide time sequence in Figure 15 reveals a gradual increase until 1300 upon which are superimposed negative excursions associated with power plant and urban plumes. For example, the mixing ratio of $H_2O_2$ in background air is ~1.0 ppbv at 1130 (UP); during transect EW1, $H_2O_2$ increases to ~1.2 ppbv at 1230 but drops to ~0.8 ppbv within plumes. This observation accords with the photochemical production mechanism, as hydroperoxide formation should turn off in the high-$NO_x$ plume environment, while hydroperoxide concentration in outside air should increase with solar intensity and ozone concentration.
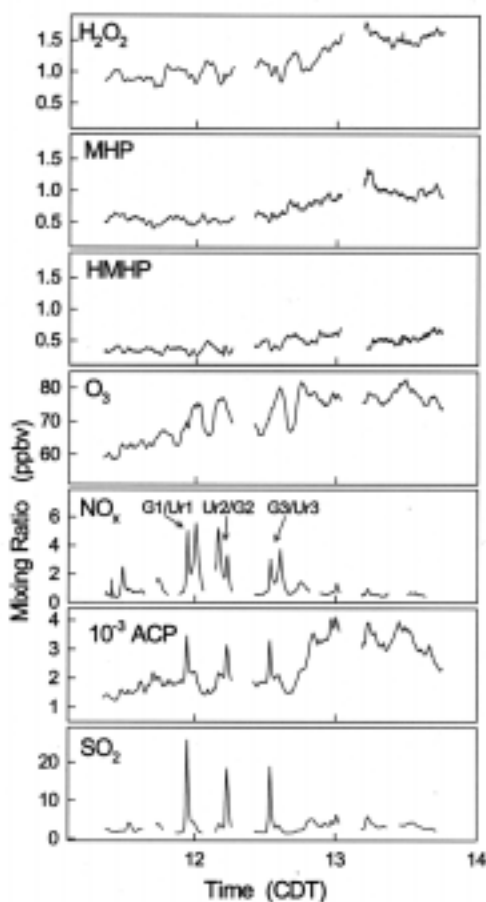
**Figure 15.** Concentrations of trace gases on July 18. All concentrations are in ppbv except ACP in particles per cubic centimeter. Peaks attributed to the Gallatin and urban plumes are noted.

A different air mass may have been sampled after 1300, based on a sharp increase in particle abundance and stabilization of ozone and hydroperoxide concentrations at that time. This flight segment, in the eastern portion of EW2, was not directly downwind of Nashville (see L. J. Nunnermacker et al., unpublished manuscript, 1998).

## 4. Discussion

Photochemical calculations were done to estimate the magnitude of in-plume hydroperoxide dips observed on July 18. For this purpose we used a constrained steady state box model, as described by *Kleinman et al.* [1997]. Using measured concentrations of $O_3$, NO, CO, HCHO, and hydroperoxides, and measured or interpolated VOC concentrations, this calculation yielded the instantaneous production and loss rates for $H_2O_2$, i.e., $P(H_2O_2)$ and $L(H_2O_2)$. The calculated net rate of change due to chemical production and loss by photolysis and reactions with OH is simply $P_{net}(H_2O_2) = P(H_2O_2)-L(H_2O_2)$. A similar calculation was performed for organic hydroperoxides to yield $P_{net}(ROOH)$. Predictions of other quantities related to $O_3$ formation are discussed in L. J. Nunnermacker et al.

(unpublished, 1998) and D. G. Imre et al. (unpublished manuscript, 1998).

Figure 16 shows measurements of $H_2O_2$ and $NO_x$ as the G-1 passed through the urban and Gallatin plumes at an altitude of 620 m (Ur1 and G1 in Figure 15). Also shown in Figure 16 is the net production rate for $H_2O_2$, calculated at 11 points on the transect immediately downwind of Nashville (EW1 in Figure 15), with a smooth curve drawn through the points. Outside of the plumes, in background air, the calculated value of $P_{net}(H_2O_2)$ is close to 0.6 ppbv h$^{-1}$. Within the plume, $H_2O_2$ production is inhibited because of high $NO_x$ concentration.
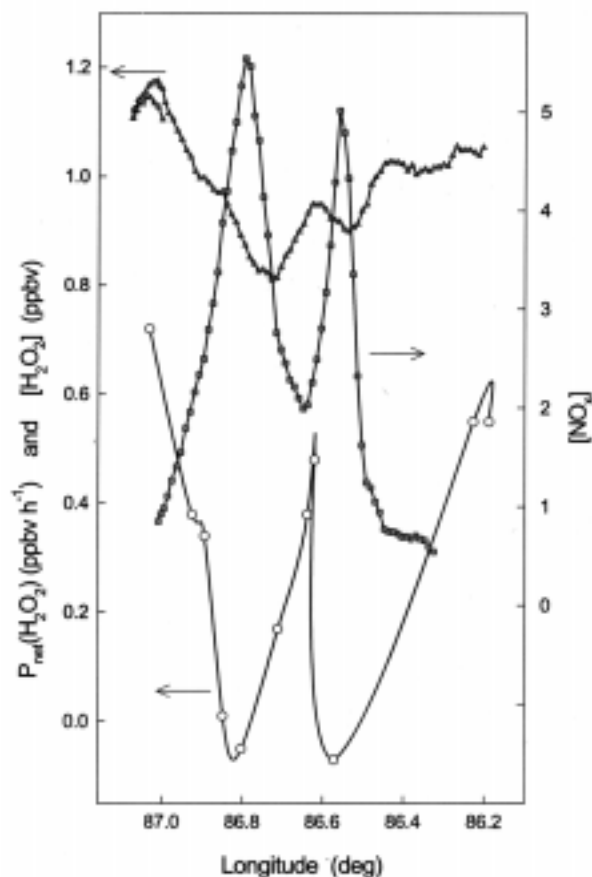


**Figure 16.** Model calculation of in-plume inhibition of peroxide formation on July 18 during EW1. Calculated $P_{net}(H_2O_2)$ (circles) includes 620 and 470 m altitudes; $NO_x$ (squares) and $H_2O_2$ (triangles) observed on 620 m transect.

This, coupled with loss by photolysis and OH reaction, results in net $H_2O_2$ destruction ($P_{net}(H_2O_2)$ = -0.06 ppbv h$^{-1}$) near the center of both plumes. These instantaneous net production rates can be used to estimate the magnitude of the in-plume dip in $H_2O_2$ concentration observed on traverse EW1. For this purpose we need to know something of the history of the background and plume air. Air that was sampled at 1215 on traverse EW1 would have passed through Nashville and the Gallatin power plant about 1.75 hours earlier, based on a 5 m s$^{-1}$ wind speed. We assume that plume air and background air had similar composition prior to encountering emission sources in Nashville and

Gallatin.  In background air, defined as $[NO_x]$ <1 ppbv, our calculations indicate that $P_{net}(H_2O_2)$ is 0.26 ppbv h$^{-1}$ at 1045 and increases linearly (slope = 0.27 ppbv r$^{-2}$, $r^2$=0.99) due to increasing solar intensity and $O_3$ mixing ratio.  This relation indicates that $H_2O_2$ in background air would increase by 0.7 ppbv during its 1.75-hour transit time.  In the plume center, a similar calculation leads to the estimate that hydroperoxide concentration would decrease by 0.1 ppbv.  The combination of the background rising by 0.7 ppbv and the plume center falling by 0.1 ppbv gives a predicted $H_2O_2$ dip of 0.8 ppbv, approximately twice that observed in Figure 16.  We do not understand the cause of this discrepancy, but note that it is consistent with the Eulerian model calculations of *Sillman et al.* [this issue] for July 18,  indicating predicted $H_2O_2$ greater than observed.

A similar calculation was done to model the observed cross-plume dip in MHP concentration.  The results are sensitive to the value of the rate coefficient k(OH+MHP) for which the recommended value (7.4 x 10$^{-12}$ cm$^3$ molecules$^{-1}$ s$^{-1}$) is an average of 2 measurements that differ by a factor of 2 [*DeMore et al.,* 1997].  We performed the calculation for several values of the rate coefficient and report here results for k = 5 x 10$^{-12}$ cm$^3$ molecules$^{-1}$ s$^{-1}$ at 298 K.  The model predicts that background air at 1030 has a calculated MHP mixing ratio of 0.55 ppbv and experiences a nearly constant net loss of MHP, $P_{net}$(MHP) = -0.005 ppbv h$^{-1}$ during its 1.75- hour trip to EW1.  At the same time, air at the plume center loses MHP at -0.12 ppbv h$^{-1}$.  This calculation predicts that a 0.20 ppbv difference in MHP mixing ratio between plume center and edges during transect EW1, compared to the observed difference of 0.15 ppbv.

## 5.  Conclusion

Hydroperoxide measurements have been presented for 12 flights of the U.S. Department of Energy G-1 aircraft during the 1995 SOS/Middle Tennessee study.  A three-channel analyzer permitted continuous measurements of $H_2O_2$, MHP, and HMHP.  Median concentration of total hydroperoxide for these flights ranged from 2.2 to 8.4 ppbv, with maximum values occurring during the stagnation episode beginning on July 11.  Photochemical hydroperoxide formation was inhibited in power plant plumes and the Nashville urban plume where $NO_x$ concentrations were high.  Individual hydroperoxide abundances were generally found in the order $H_2O_2$ > MHP > HMHP, with organic hydroperoxides constituting more than 50% of the total.  Vertical profiles of HMHP showed higher concentrations near the ground, consistent with a formation mechanism involving biogenic alkenes.  A free radical source for all three hydroperoxides is indicated by their profiles in the free troposphere, which generally track the profiles of ozone and water vapor.

This study confirms predictions that organic hydroperoxide may constitute a large fraction of total hydroperoxide under some conditions [*Logan et al.,* 1981].  Using the three-channel analyzer, we have observed predominantly $H_2O_2$ in Nova Scotia and Long Island, New York, but larger fractions of HMHP and MHP in Atlanta and Metter, Georgia, and in Nashville.  High temperature, humidity, and contributions from biogenic hydrocarbons in the South may contribute to higher organic hydroperoxide production there.  Few hydroperoxide measurements have been conducted in the southeastern United States.  One set of measurements, conducted in summer at a high elevation site in North Carolina, showed mean $H_2O_2$ below 1 ppbv [*Claiborn*

*and Aneja,* 1991; *Aneja et al.,* 1994].  Mean $H_2O_2$ concentration also remained below 1 ppbv at a rural site in the Piedmont region of North Carlina despite a peak afternoon temperature of 35°C (Das and Aneja, 1994).  These studies found that organic hydroperoxides constituted less than 20% of total hydroperoxide, although the accuracy of HMHP determination using *p*OHPAA/HRP reagent has been questioned [*Kurth et al.,* 1991].  These observations underscore the importance of further development of field measurement techniques for hydroperoxides, of validating the kinetics of individual organic hydroperoxide sources and sinks, and of including molecular ozone-alkene formation pathways in photochemical models.

## References

Aneja, V.P., C.S. Claiborn, Z. Li, and A. Murthy, Trends, seasonal variations and analysis of high altitude surface nitric acid, ozone and hydrogen peroxide, *Atmos. Environ.*, *28* , 1781-1790, 1994.

Ayers, G.P., S.A. Penkett, R.W. Gillett, B. Bandy, I.E. Galbally, C.P. Meyer, C.M. Elsworth, S.T. Bentley, and B.W. Forgan, The annual cycle of peroxides and ozone in marine air at Cape Grim, Tasmania, *J. Atmos. Chem.*, *23*, 221-252, 1996.

Barth, M.C., D.A. Hegg, P.V. Hobbs, J.G. Walega, G.L. Kok, B.G. Heikes, and A.L. Lazrus, Measurements of atmospheric gas-phase and aqueous-phase hydrogen peroxide concentrations in winter on the east coast of the United States, *Tellus*, *Ser. B, 41*, 61-69, 1989.

Becker, K.H., K.J. Brockman, and J. Bechara, Production of hydrogen peroxide in forest air by reaction of ozone with terpenes, *Nature, 346*, 256-258, 1990.

Claiborn, C., and V.P. Aneja, Measurements of atmospheric hydrogen peroxide in the gas phase and in cloud water at Mt. Mitchell, North Carolina, *J. Geophys. Res.*, *96* , 18,771-18,787, 1991.

Das, M., and V.P. Aneja, Measurements and analysis of concentrations of gaseous hydrogen peroxide and related species in the rural central Piedmont region of North Carolina, *Atmos. Environ.*, *28* 2473-2483, 1994.

Daum, P.H., L.I. Kleinman, A.J. Hills, A.L. Lazrus, A.C.D. Leslie, K. Busness, and K. Boatman, Measurement and interpretation of concentrations of $H_2O_2$ and related species in the upper Midwest during summer, *J. Geophys. Res.*, *95*, 9857-9871, 1990.

DeMore, W.B., S.P. Sander, D.M. Golden, R.F. Hampson, M.J. Kurylo, C.J. Howard, A.R. Ravishankara, C.E. Kolb, and M.J. Molina, Chemical kinetics and photochemical data for use in stratospheric modeling, *Eval. 12*, NASA, Jet Propul. Lab., Calif. Inst. of Technol., Pasadena, 1997.

Enders, G., et al., Biosphere/atmosphere interactions: Integrated research in a European coniferous forst ecosystem, *Atmos. Environ.*, *Ser. A, 26*, 171-189, 1992.

Ennis, C.A., A.L. Lazrus, P. Zimmerman, and R.K. Monson, Flux determinations and physiological response in the exposure of red spruce to gaseous hydrogen peroxide, ozone and sulfur dioxide, *Tellus*, *Ser. B, 42*, 183-199, 1990.

Fels, M., and W. Junkermann, The occurrence of organic peroxides in air at a mountain site, *Geophys. Res. Lett.*, *21*, 341-344, 1994.

Gäb, S., W.V. Turner, S. Wolff, K.H. Becker, L. Ruppert, and K.J. Brockmann, Formation of alkyl and hydroxyalkyl hydroperoxides on ozononlysis in water and air, *Atmos. Environ.*, *29* , 2401-2407, 1995.

Guenther, A.B., P.R. Zimmerman, and P.C. Harley, Isoprene and monoterpene emission rate variability:  Model evaluations and sensitivity analysis, *J. Geophys. Res.*, *98*, 12,609-12,617, 1993.

Heikes, B., et al., Ozone, hydroperoxides, oxides of nitrogen, and hydro-carbon budgets in the marine boundary layer over the South Atlantic, *J. Geophys. Res.*, *101*, 24,221-24,234, 1996.

Heikes, B.G., G.L. Kok, J.G. Walega, and A.L. Lazrus, $H_2O_2$, $O_3$, and $SO_2$ measurements in the lower troposphere over the eastern United States during Fall, *J. Geophys. Res.*, *92*, 915-931, 1992.

Hellpointner, E., and S. Gäb, Detection of methyl, hydroxymethyl and hydroxyethyl peroxides in air and precipitation, *Nature, 337*, 631-634, 1989.

Hewitt, C.N., and G.L. Kok, Formation and occurrence of organic peroxides in the troposphere: Laboratory and field observations, *J. Atmos. Chem.*, *12*, 181-194, 1991.

Hübler, G., et al., An overview of the airborne activities during the SOS 1995 Nashville/Middle Tennessee Ozone Study, *J. Geophys. Res.*, *this issue*.

Jacob, D.J., L.W. Horowitz, J.W. Munger, B.G. Heikes, R.R. Dickerson, R.S. Artz, and W.C. Keene, Seasonal transition from $NO_x$ - to hydro-carbon-limited conditions for ozone prodcution over the eastern United States in September, *J. Geophys. Res.*, *100*, 9315-9324, 1995.

Kleinman, L.I., Photochemical formation of peroxides in the bounary layer, *J. Geophys. Res.*, *91*, 10,889-10,904, 1991.

Kleinman, L.I., P.H. Daum, Y.-N. Lee, J.H. Lee, L.J. Nunnermacker, S.R. Springston, L. Newman, J. Weinstein-Lloyd, and S. Sillman, Dependence of ozone production on NO and hydrocarbons in the troposphere, *Geophys. Res. Lett.,24* (18), 2299-2302, 1997.

Kok, G.L., K. Thompson, A.L. Lazrus, and S.E. McLaren, Derivatization technique for the determination of peroxides in precip-itation, *Analytical Chemistry, 58*, 1192-1194, 1986.

Kok, G.L., J.G. Walega, B.G. Heikes, J.A. Lind, and A.L. Lazrus, Measurements of hydrogen peroxide and formaldehyde in Glendora, CA, *Aerosol Science and Technology*, *12*, 49-55, 1990.

Kurth, H.-H., S. Gab, W.V. Turner, and A. Kettrup, A high-performance liquid chromatography system with an immobilized enzyme reactor for detection of hydrophilic organic peroxides, *Anal. Chem.*, *63*, 2586-2589, 1991.

Lazrus, A.L., G.L. Kok, J.A. Lind, S.N. Gitlin, B.G. Heikes, and R.E. Shetter, Automated fluorometric method for hydrogen peroxide in air, *Analytical Chemistry*, *58*, 594-597, 1986.

Lee, J. H., D. F. Leahy, I. N. Tang, and L. Newman, Measurement and speciation of gas-phase peroxides in the atmosphere, *J. Geophys. Res.*, *98*, 2911-2915, 1993.

Lee, J.H., I.N. Tang, and J.B. Weinstein-Lloyd, Nonenzymatic method for the determination of hydrogen peroxide in atmospheric samples, *Analytical Chemistry*, *62*, 2381-2384, 1990.

Lee, J.H., I.N. Tang, J.B. Weinstein-Lloyd, and E.B. Halper, An improved nonenzymatic method for the determination of gas-phase peroxides, *Environ. Sci. Technol.*, *28*, 1180-1185, 1994.

Lee, Y.N., et al., Atmospheric chemistry and distribution of formalde-hyde and several multi-oxygenated carbonyl compounds during the 1995 Nashville/Middle Tennessee Ozone Study, *J. Geophys. Res.*, *this issue.*

Lind, J.A., and G.L. Kok, Correction to "Henry's law determinations for aqueous solutions of hydrogen peroxide, methyl hydroperoxide and peroxyacetic acid" by John A. Lind and Gregory L. Kok, *J. Geophys. Res.*, *99*, 21,119, 1994.

Lind, J.A., A.L. Lazrus, and G.L. Kok, Aqueous phase oxidation of sulfur(IV) by hydrogen peroxide, methyl hydroperoxide and peroxy-acetic acid, *J. Geophys. Res.*, *92,* 4171-4177, 1987.

Logan, J.A., M.J. Prather, S.C. Wofsy, and M.B. McElroy, Tropospheric chemistry; A global perspective, *J. Geophys. Res.*, *86*, 7210-7254, 1981.

Macdonald, A.M., K.G. Anlauf, C.M. Banic, W.R. Leaitch, and H.A. Wiebe, Airborne measurements of aqueous and gaseous hydrogen peroxide during spring and summer in Ontario, Canada, *J. Geophys. Res.*, *100*, 7253-7262, 1995.

Madronich, S., and J.G. Calvert, Permutation reactions of organic peroxy radicals in the troposhere, *J. Geophys. Res.*, *95*, 5697-5715, 1990.

Martin, R.S., H. Westberg, E. Allwine, L. Ashman, J.C. Farmer, and B. Lamb, Measurement of isoprene and its atmospheric oxidation products in a central Pennsylvania deciduous forest, *J. Atmos. Chem.*, *13*, 1-32, 1991.

Masuch, G., A. Kettrup, R.K.A.M. Mallant, and J. Slanina, Effects of $H_2O_2$ - containing acidic fog on young trees, *Environ. Anal. Chem.*, *27*, 183-213, 1986.

McNider, R.T., W.B. Norris, A.J. Song, R.L. Clymer, S. Gupta, R.M. Banta, R.J. Zamora, A.B. White, and M. Trainer, Meteorological conditions during the 1995 SOS Nashville/Middle Tennessee Field Intensive, *J. Geophys. Res.*, this issue.

Penkett, S.A., B.M.R. Jones, K.A. Brice, and A.E.J. Eggleton, The importance of atmospheric ozone and hydrogen peroxide in oxidizing sulfur dioxide in cloud and rain water, *Atmos. Environ.*, *13*, 123-137, 1979.

Sillman, S., The use of $NO_y$, $H_2O_2$, and $HNO_3$ as indicators for ozone-$NO_x$-hydrocarbon sensitivity in urban locations, *J. Geophys. Res.*, *100*, 14,175-14,188, 1995.

Sillman, S., et al., Photochemistry of ozone formation in Atlanta, GA: Models and measurements, *Atmos. Environ.*, *29*, 3055-3066, 1995.

Sillman, S., D. He, M. Pippin, P.H. Daum, D. G. Imre, L. Kleinman, J.H. Lee, and J. Weinstein-Lloyd, Model correlations for ozone, reactive nitrogen and peroxides for Nashville in comparison with measurements: Implications for $O_3$-$NO_x$-hydrocarbon chemistry, *J. Geophys. Res.*, this issue.

Tanner, R.L., and D.E. Schorran, Measurements of gaseous peroxides near the Grand Canyon - Implication for summertime visibility impairment from aqueous-phase secondary sulfate formation, *Atmos. Environ.*, *29*, 1113-1122, 1995.

Tremmel, H.G., W. Junkermann, and F. Slemr, Distribution of organic peroxides during aircraft measurements over the northeastern United States, *J. Geophys. Res.*, *99* , 5295-5307, 1994.

Tremmel, H.G., W. Junkrmann, F. Slemr, and U. Platt, On the distribu-tion of hydrogen peroxide in the lower troposphere over the north-eastern United States during late summer 1988, *J. Geophys. Res.*, *98*, 1083-1099, 1993.

Weinstein-Lloyd, J., P.H. Daum, L.J. Nunnermacker, J.H. Lee, and L.I. Kleinman, Measurement of peroxides and related species in the 1993 North Atlantic Regional Experiment, *J. Geophys. Res.*, *101*, 29,081-29,090, 1996a.

Weinstein-Lloyd, J., J.H. Lee, P.H. Daum, B.T. Jobson, and D.D. Parrish, Intercomparison of peroxide data from the DOE G-1 and NOAA P-3 aircraft during the 1995 Nashville SOS study, *EOS Trans. AGU*, *77* (46), Fall Meet. Suppl., F97, 1996b.

Weller, R., and O. Schrems, $H_2O_2$ in the marine troposphere and seawater of the Atlantic Ocean, *Geophys. Res. Lett.*, *20*, 125-128, 1993.

Zhou, X., and Y.-N. Lee, Aqueous solubility and reaction kinetics of hydroxymethyl hydroperoxide, *J.Phys.Chem.*, *96*, 265-272, 1992.

———

J. B. Weinstein-Lloyd, Chemistry/Physics Department, State University of New York, Old Westbury, NY 11568. (e-mail: jlloyd@bnl.gov)

J. H. Lee, P. H. Daum, L. I. Kleinman, L. J. Nunnermacker, S. R. Springston, and L. Newman, Environmental Chemistry Division, Department of Applied Science, Brookhaven National Laboratory, Upton, NY 11973-5000.